Jour. Korean Earth Science Society, v. 28, no. 5, p. 613-619, September 2007

# A Numerical Study on the Formation Mechanism of a Mesoscale Low during East-Asia Winter Monsoon

**Hyun-Suk Koo[1], Hae-Dong Kim[1,*], Sung-Dae Kang[2], and Dong-Wook Shin[3]**

[1]Department of Environmental Conservation and Disaster Prevention Keimyung University, Daegu 704-701, Korea

[2]Climate Prediction Division, Korea Meteorological Administration, Seoul 156-720, Korea

[3]Center for Ocean-Atmospheric Prediction Studies (COAPS), Florida State University, FL 32306-2840, USA

**Abstract:** Mesoscale low is often observed over the downstream region of the East Sea (or, northwest coast off the Japan Islands) during East-Asia winter monsoon. The low system causes a heavy snowfall at the region. A series of numerical experiments were conducted with the aid of a regional model (MM5 ver. 3.5) to examine the formation mechanism of the mesoscale low. The following results were obtained: 1) A well-developed mesoscale low was simulated by the regional model under real topography, NCEP reanalysis, and OISST; 2) The mesoscale low was simulated under a zonally averaged SST without topography. This implies that the meridional gradient of SST is the main factor in the formation of a mesoscale low; 3) A thermal contrast (>10°C) of land-sea and topography-induced disturbance served as the second important factor for the formation; 4) Paektu Mountain caused the surface wind to decelerate downstream, which created a more favorable environment for thermodynamic modification than that was found in a flat topography; and 5) The types of cumulus parameterizations did not affect the development of the mesoscale low.

Keywords: Mesoscale circulation, Mountain effect, MM5, SST Forcing, East-Asia winter monsoon

## Introduction

Well-developed mesoscale lows have been frequently observed during East-Asia winter monsoon. Many meteorologists and forecasters have studied the mechanism of mesoscale low because they cause heavy snowfall on the northwest coast off the Japan Islands.

Fig. 1a shows the surface weather chart at 12UTC on January 23, 1990. A well-developed mesoscale low with the recorded central pressure of 1010 hPa is shown around the northwest coast of the Japan Islands. There is a cold air-outbreak from the Korean Peninsula to the Japan Islands. As the cold air advects from the Korean Peninsula to the Japan Islands or the East Sea, the thermodynamic properties of the atmospheric boundary layer are changed because of heating from the East Sea. The maximum altitude in the upstream region is 2.8 km at Paektu Mountain. The typical Froude number at the upstream region is about 0.23 during the cold-air outbreak. Therefore, one can expect the meandering of flow passing through mountain. A series of mesoscale vortices caused by the meandering flow can be seen in the satellite image at the downstream region.

Numerical studies on the mesoscale vortices over the East Sea have been carried out by Ninomiya (1989) and Nagata (1991). Ninomiya (1989) made a systematic study on the polar and/or comma-cloud (P/C) cyclone over the East Sea in winter. According to the results of those studies, a strong low-level baroclinicity caused by the surface fluxes is primarily important for the formation of P/C.

Nagata (1991) carried out a series of numerical experiments on the formation of the convergent cloud band (CCB) over the East Sea in winter. He concluded that the three lower boundary forcings, which include the land-sea thermal contrast, the blocking effect of the mesoscale mountains located in the north of the Korean Peninsula, and the characteristic SST distribution with large gradients along 40°N, are comparably important for the

*Corresponding author: khd@kmu.ac.kr
Tel: 82-53-580-5930
Fax: 82-53-580-5385

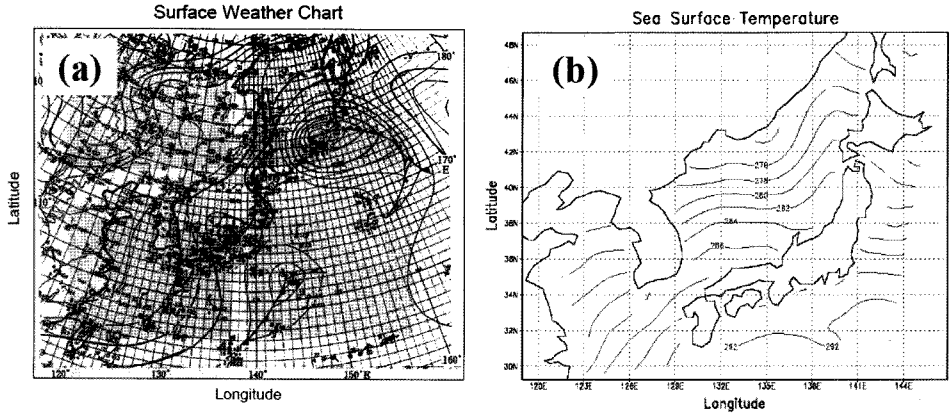


**Fig. 1.** (a) Synoptic surface map at 12 UTC 23 January 1990. There is a well-developed mesoscale low near northwest coast of the Japan Islands. The central pressure of the mesoscale low is 1010 hPa. (b) Spatial distribution of sea surface temperature at 12 UTC 23 January 1990. There is zonally homogeneous distribution of SST between 35°N and 42°N.

formation of a mesoscale low.

There have been many studies on the interpretation of mechanical disturbances around topography with a low Froude number (Smolarkiewicz and Rotunno, 1989; Olafsson and Bougeault, 1996; Kang and Kimura, 1997, 1998). These studies suggested that the vortex formation in the lee of an isolated mountain is derived from an isentropic deformation (Smolarkiewicz and Rotunno, 1989), the breaking of a mountain wave (Olafsson and Bougeault, 1996) and the divergence of the vertical momentum flux (Kang and Kimura, 1998). The geographical distance between a mesoscale low and the upstream region of a mountain (Paektu Mountain) is about 900km (see Fig. 1a). Based on these theories, however, it is difficult to explain the formation mechanism of a mesoscale-low-related vortex that is located far from the upstream region of a mountain. Another forcing mechanism, such as the thermal disturbance caused by warm SST, might be required to explain the formation mechanism of a mesoscale low.

Kang and Kimura (1997) studied the effects of both mechanical and thermal disturbances on the formation of cloud streets in the lee of an isolated mountain near a coast. They carried out a series of numerical experiments for the different static instabilities over a warm sea surface. They also conducted experiments to study the effect of an upstream mountain on the formation of cloud streets. According to the results, both disturbances are important for the formation of well-developed cloud streets in the lee of an isolated mountain during a winter season. The main energy source maintaining the convective roll was sensible heat from warm seas surface, and the release of latent heat in the cloud was minor energy source.

Tsuboki and Asia (2004) carried out a simulation and sensitivity experiments with respect to several forcing factors to elucidate the development mechanism of mesoscale lows. According to these results, the diabatic heating due to condensation, vertical diffusion of the sensible heat, and horizontal advection of the potential temperature are almost in balance with the negative vertical advection of potential temperature. This resulted in an intense upward motion in the convergence zone. However, it is not clearly mentioned about the main energy source causing the intense upward motion.

Despite specific numerical studies carried out on the formation mechanism of a mesoscale low, they do not sufficiently explain the phenomenon. Another forcing, such as a meridionally gradient of SST, might be important for the formation of a mesoscale low. To estimate the formation mechanism of a mesoscale low by using a regional model, a series of numerical experiments were conducted in this study (see Table 1).

Section 2 presents the model description and the

**Table 1.** List of numerical experiment cases

| Cases | Topography | SST | Meridional Gradient of SST | Mesolow |
|---|---|---|---|---|
| CTL | real topography | real SST | 9°C | ○ |
| RZ | real topography | zonal mean SST | 7°C | ○ |
| FR | flat topography | real SST | 9°C | ○ |
| FZ | flat topography | zonal mean SST | 7°C | ○ |
| RU03 | real topography | uniform SST (03°C) | 0°C | × |
| RU12 | real topography | uniform SST (12°C) | 0°C | × |

Remark: The meridional gradient of SST is estimated between 36°N and 42°N at 135°E.

design of numerical experiments. The formation mechanism of a mesoscale low is given in Section 3. The summary and conclusion are presented in Section 4.

## Model Description and Design of the Numerical Experiment

### Model descriptions

The NCAR MM5 (Grell et al., 1993) is used as a numerical model in this study. To investigate the formation mechanism of mesoscale low, it is very important to set up every physical option appropriately in the MM5 configurations such as cumulus convection, PBL, microphysics, and radiation. The selected options for cumulus convection, PBL, microphysics, and radiation are the Kain-Fritsch scheme (Kain and Fritsch, 1993), MRF PBL (Hong and Pan, 1996), simple ice (Dudhia, 1989) and the CCM2 radiation scheme (Hack et al., 1993), respectively.

### Designs of numerical experiments

The NCEP reanalysis data (6-hour intervals, 2.5deg × 2.5deg) are used as the initial and lateral boundary conditions for this study. The boundary conditions of the ocean surface are given by weekly NCEP-OISST (1.0deg × 1.0deg). The standard MM5 preprocessor was used to prepare the initial and boundary conditions. The numbers of horizontal grid-points are 52 × 52 and 51 × 51 for the mother and nesting domains, respectively. Their horizontal grid intervals are 120 km and 40 km, respectively. The model atmosphere extends up to 25 km in the vertical direction and is divided into 23 layers with coarser resolution progressively upward.

The list of numerical experiments in this study is shown in Table 1. The CTL is the control case for this study. To estimate the effects of SST and topography-induced disturbances, three (RZ, RU03, and RU12) and two (FR and FZ) numerical experiments were conducted, respectively. RZ means that the experiment was conducted under real topography and zonally averaged SST. RU03 and RU12 mean real topography with uniform distribution of 3.0°C and 12.0°C of SST, respectively. FR and FZ indicate flat topography (10 m) with real and zonally averaged SST, respectively.

## Formation Mechanism of a Mesoscale Low

The spatial distribution of SST is shown in Fig. 1b. There are zonally homogeneous and nonhomogeneous of SST at region I (35°N-42°N, 129°E-140°E) and region II (42°N-49°N, 129°E-140°E) respectively. The two different distributions of SST show that there are strong thermal fluxes in the downstream regions, i.e., the location of the mesoscale low, and a strong thermal contrast between land and sea in the upstream region. The estimated value of a meridional SST-gradient between 36°N and 42°N at 135°E is about 9.0°C. The thermal contrast between land and sea along 135°E is about 9.0°C.

Fig. 2 shows the simulated sea-level pressure and wind vector for two numerical experiments (CTL and RZ; see Table 1). The triangular mark placed in the north of the Korean Peninsula is Paektu Mountain.

The CTL case is shown in Fig. 2a. The simulated pressure field of the CTL case closely resembles that

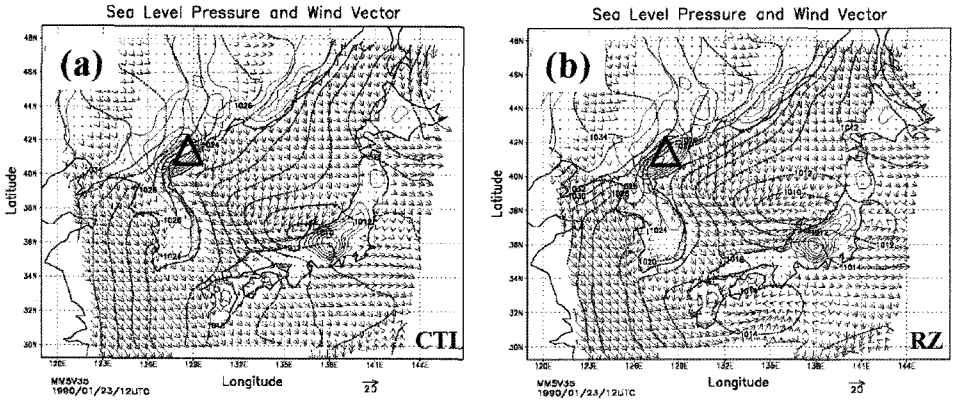


**Fig. 2.** Simulated sea level pressure and wind field for CTL case (a) and RZ case (b) at 12 UTC 23 January 1990, respectively.

shown in Fig. 1a. The central pressure of the mesoscale low in both figures is about 1010hPa. This means that the CTL case accurately recaptures the observed mesoscale characteristics. As mentioned in Table 1, the CTL case considers topography-induced mechanical and SST induced thermal disturbances simultaneously. Therefore, it is unclear which disturbance is dominant for the formation of a mesoscale low. To investigate the relative contribution of both disturbances on the formation of a mesoscale low, it will be necessary to separate one from the other in numerical experiments.

As Nagata (1991) mentioned, the characteristic SST distribution with large gradients along 40°N is comparably important for the formation of a mesoscale low around the East Sea. Especially, the meridional gradient of SST in winter is significantly larger than that in summer.

To see the details of the effect of meridional gradient of SST, a numerical experiment (RZ case) under a zonal mean SST with topography was conducted. The numerical result of the RZ case is shown in Fig. 2b. The mesoscale low is simulated under the zonal mean SST with topography.

A comparison of CTL and RZ shows that the location(the northwest coast of the Japan Islands) and central pressure (1010hPa) of mesoscale low are similar in each case.

This means that a zonal mean SST provides favorable thermal fluxes for the formation of a mesoscale low from the warm sea surface. To separate the effect of topography-induced mechanical disturbance from an RZ case (see Fig. 2b), two numerical experiments (FR case and FZ case) were conducted in flat topography.

Fig. 3 shows the simulated mesoscale low in flat topography. Fig. 3a shows the simulated sea level pressure and wind vector in flat topography and real SST (FR case; see Table 1). Even though the cyclonic flow and pressure pattern are not clear at the same time of weather map (see Fig. 1a), however, Fig. 3a shows a little bit organized mesoscale low in flat topography and real SST. The cyclonic flow and low-pressure system intensified as time elapsed.

Fig. 3b shows the simulated mesoscale low in flat topography and zonal mean SST (FZ case; see Table 1). The mesoscale low can be seen at almost the same location but with slightly reduced strength. This means that the effect of a topography-induced mechanical disturbance is not the main factor in the formation of a mesoscale low.

According to the comparison shown in Fig. 2b and Fig. 3b, the meridional gradient of SST is the main factor in the formation of the mesoscale low. Even though the topography-induced disturbance is not the main factor in the formation of a mesoscale low, the comparison of CTL (see Fig. 2a) and FZ (see Fig. 3b) shows that the mechanical disturbance enforces the strength of a mesoscale low. The location of a mesoscale low in the case of FZ shifted slightly to the northeast.

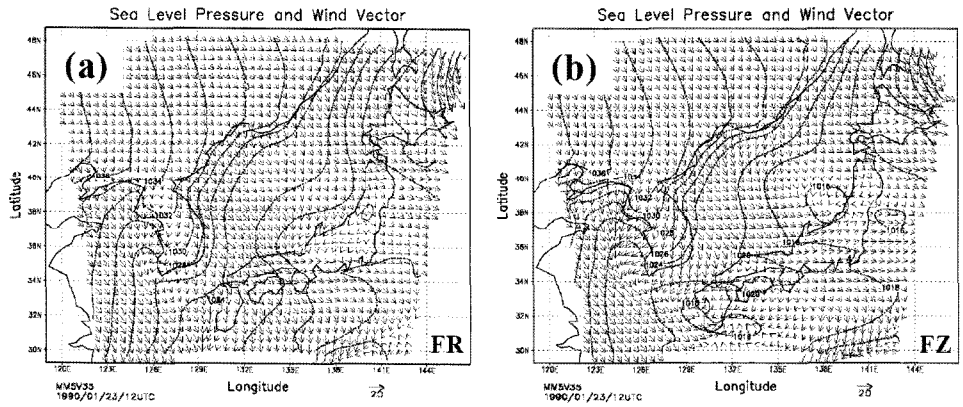


**Fig. 3.** Same as Fig. 2, except for FR case (a) and FZ case (b), respectively.

Considering the results from the three numerical experiments above (in the cases of CTL, RZ, and FZ), the meridional gradient of SST is the main factor in the formation of a mesoscale low around the northwest coast of the Japan Islands during winter monsoon. The thermal contrast of a land-sea and topography-induced disturbance are the second important elements in the formation.

To estimate the effect of downstream blocking of the topography (Japan Islands), two additional numerical experiments were conducted (not shown here). The topography in each case was the same as that shown in Fig. 3, except for the existence of downstream topography (Japan Islands) in the numerical domains.

According to the results, the existence of a downstream mountain under real SST intensified the mesoscale low by a decrease of about 2hPa of central pressure. However, the mesoscale low was weakened under a zonal mean SST by an increase of about 4hPa of central pressure.

To clarify the importance of a meridional SST-gradient for the formation of a mesoscale low, two more numerical experiments (RU03 and RU12 cases) were conducted under uniform distributions of SST over the East Sea.

The results of the numerical experiments under real topography but with an uniform SST given as 3.0°C (RU03 case) and 12.0 (RU12 case) are shown in Fig. 4. The effects of uniformly supplied thermal fluxes from the East Sea are shown in this figure. There is no mesoscale low in the RU03 case (see Fig. 4a). As the SST increases uniformly, a type of thermal low is generated (see Fig. 4b). However, the location and central pressure are different from CTL case. The location of the mesoscale low in the case of RU12 shifts further to the northeast than it does in the case of CTL (see Figs. 2a and 4b). This means that the existence of a meridional SST-gradient is the main factor for the correct location and strength of a mesoscale low, as shown in the synoptic weather map (see Fig. 1a).

The importance of the mechanical disturbance can be understood through the trajectory analysis of an advecting air parcel from Paektu Mountain to the northwest coast of the Japan Islands. Its importance can be explained by the process of the air parcel's thermodynamic modification over the sea surface. To see the process, trajectory analysis in the case of CTL (real topography with real SST) and FR case (flat topography with real SST) was conducted by releasing several parcels at the upstream region (not shown here). The traveling time between Paektu Mountain and the center of the mesoscale low was calculated. According to the results, the traveling times are about 18 hours and 21 hours for CTL case and FR case. The presence of the Paektu Mountain increases the traveling times by about 3 hours. This means that Paektu Mountain decelerates the surface wind speed and provides a more favorable environment of

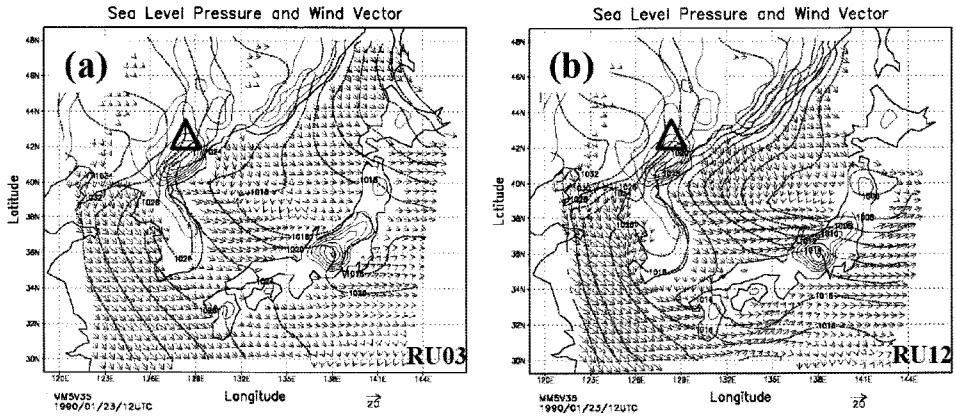


**Fig. 4.** Same as Fig. 2, except for RU03 case (a) and RU12 case (b), respectively.

thermodynamic modification than flat topography does. Due to such reason, in case of CTL (see Fig. 2a), the mesoscale low was better developed than it was in case of FR (see Fig. 3a). However, the comparison of RZ (see Fig. 2b) and FZ (see Fig. 3b) shows that the mesoscale low can develop under the meridional SST gradient only, which is to say that the decelerated wind speed caused by Paektu Mountain is not necessary. This means that the existence of a meridional SST gradient is a more dominant factor than the decelerated flow caused by Paektu Mountain for the development of a mesoscale low. The decelerate wind speed also contribute to the formation of a mesoscale low, however, as the second important factor.

## Summary and Conclusion

The mesoscale low frequently observed at the downstream region of the East Sea (or, Northwest coast region of Japan Islands) during winter monsoon. It is difficult to explain the formation mechanism of the lee vortex related to a mesoscale low because of the geographical distance (900 km) between the mesoscale low and the upstream region of Paektu Mountain, which is too far to form the vortex (Smolarkiewicz and Rotunno, 1989; Olafsson and Bougeault, 1996; Kang and Kimura, 1997, 1998). Another forcing mechanism, such as the SST-induced disturbance, might be required to explain the formation mechanism of the mesoscale low.

In this study, the development mechanism of a mesoscale low was examined by numerical experiments using a regional model (MM5 version 3.5). To estimate the formation mechanism of a mesoscale low, a series of numerical experiments was conducted (see Table 1).

Well-developed mesoscale low was simulated by a regional model under real topography, NCEP reanalysis, and OISST. The mesoscale low was simulated under the meridional gradient of SST (i.e., under the strong thermal fluxes over the western part of the Japan Islands), but no topography was used. This means that the topographically induced mechanical disturbance is not a main factor in the formation of mesoscale low. The thermal contrast (>10°C) of the land-sea and topography-induced disturbance is the second important element.

The presence of a mountain in the upstream region under real SST and zonal mean SST intensifies the strength of a mesoscale low, and the strength decreases in the absence of a mountain.

Paektu Mountain increases the traveling time between Paektu Mountain and the center of mesoscale low by about 3 hours. This means that the presence of Paektu Mountain decelerates the surface wind speed and provides a more favorable environment for thermodynamic modification than flat topography does.

The schemes of cumulus parameterizations (Kuo, Arakawa-Shuberthz, Mett-Mellor, Kain-Frisher, Direct simulation) did not affect the development of the mesoscale low.

## Acknowledgments

"This work was supported by the Korea Research Foundation Grant funded by the Korean Government (MOEHRD)" (KRF-2006-C00696)

## References

Dudhia, J., 1989, Numerical study of convection observed during the winter Monsoon experiment using a mesoscale two-dimensional model. Journal of the Atmospheric Sciences, 46 (20), 3077-3107.

Grell, G.A., Dudhia, J., and Stauffer, D.R., 1993, A description of the fifth generation Penn State/NCAR mesoscale model. NCAR Tech. Note, 398+IA, 122 p.

Hack, J.J., Boville, B.A., Briegleb, B.P., Kiehl, J.T., Rasch, P.J., and Williamson, D.L., 1993, Description of the NCAR community Climate Model (CCM2). NCAR Technical Note, NCAR/TN-382+STR, 120 p.

Hong, S.Y. and Pan, H.L., 1996, Nonlocal boundary layer vertical diffusion in a medium-range forecast model. Monthly Weather Review, 124 (10), 2322-2339.

Kain, J.S. and Fritsch, J.M., 1993, Convective parameterization for mesoscale models: The Kain-Fritsch Scheme. The Representation of Cumulus Convection in Numerical Models, Meteorological Monographs, 46, 165-170.

Kang, S.D. and Kimura, F., 1997, A numerical study on the mechanism of Cloud-Street formation in the lee of an isolated mountain near a coast. Journal of Meteorological Society of Japan, 75, 955-968.

Kang, S.D. and Kimura, F., 1998, A numerical study on the Karman vortex generated by divergence of momentum flux in flow past an isolated mountain. Journal of Meteorological Society of Japan, 76, 925-935.

Nagata, M., 1991, Further numerical study on the formation of the convergent cloud band over the Japan Sea in winter. Journal of Meteorological Society of Japan, 69, 419-427.

Ninomiya, K., 1989, Polar/comma-cloud lows over the Japan Sea and the Northwestern Pacific in winter. Journal of Meteorological Society of Japan, 67, 83-97.

Olafsson, H. and Bougeault, P., 1996, Nonlinear flow past and elliptic mountain ridge. Journal of Meteorological Society of Japan, 53, 2465-2489.

Smolakiewicz, P.K. and Rotunno, R., 1989, Low Froude number flow past three-dimensional obstacles. Part I: Baroclinically generated lee vortices. Journal of the Atmospheric Sciences, 46, 1154-1164.

Tsuboki, K. and Asai, T., 2004, The multi-scale structure and development mechanism of mesoscale lows over the Sea of Japan in winter. Journal of Meteorological Society of Japan, 82, 597-621.

Manuscript received: 9 April 2007
Revised manuscript received: 27 August 2007
Manuscript accepted: 14 September 2007